ADP-Ribosylation of Cyclophilin A by *Pseudomonas aeruginosa* Exoenzyme S

Augustine A. DiNovo,[‡] Kevin L. Schey,[§] William S. Vachon,[||] Eileen M. McGuffie,[⊥] Joan C. Olson,*[,#] and Timothy S. Vincent[#]

Departments of Pathology and Laboratory Medicine, Cell and Molecular Pharmacology, and Experimental Therapeutics, Medical University of South Carolina, Charleston, South Carolina 29425, Department of Microbiology, Immunology and Cell Biology, West Virginia University, School of Medicine, Morgantown, West Virginia 26506, Department of Biology, Coastal Carolina University, Conway, South Carolina 29528, and Department of Biology, College of Charleston, Charleston, South Carolina 29424

Received July 13, 2005; Revised Manuscript Received February 9, 2006

ABSTRACT: The virulence of the opportunistic pathogen *Pseudomonas aeruginosa* (*Pa*) is in part mediated by the type III secretion (TTS) of bacterial proteins into eukaryotic hosts. Exoenzyme S (ExoS) is a bifunctional *Pa* TTS effector protein, with GTPase-activating (GAP) and ADP-ribosyltransferase (ADPRT) activities. Known cellular substrates of TTS-translocated ExoS (TTS-ExoS) ADPRT activity include proteins in the Ras superfamily and ERM family proteins. This study describes the ADP-ribosylation of a non-G-protein substrate of TTS-ExoS, cyclophilin A (CpA), a peptidyl-prolyl isomerase (PPIase). Four novel 17 kDa proteins (p*I* 6.5−6.8) were recognized in a proteomic screen of lysates of human epithelial cells that had been exposed to ExoS-producing *Pa*, but not an isogenic non-ExoS producing strain. The proteins were identified as isoforms of CpA using MALDI-TOF mass spectrometry and confirmed by Western blotting. Mutagenesis analysis identified arginine 55 and 69 of CpA as sites of ExoS ADP-ribosylation. Examination of the effect of ExoS ADP-ribosylation on CpA function found a moderate (19%) decrease in prolyl isomerization of a Xaa-Pro containing peptides. In comparison, GST-CpA co-immunoprecipitation studies found ExoS ADP-ribosylation of CpA to efficiently inhibit CpA binding to calcineurin/PP2B phosphatase. Our results support that ExoS ADP-ribosylates and affects the function of the cytosolic protein, CpA, with the predominant functional effect relating to interference of CpA-cellular protein interactions.

Pseudomonas aeruginosa is an opportunistic pathogen with the ability to cause life-threatening infection to individuals with compromised immunity, cystic fibrosis, or extensive burns or wounds (*1*). The pathogenesis of *Pa* relates to its regulated production of multiple virulence factors, one of which is the TTS-effector, ExoS. Direct contact of *Pa* with eukaryotic cells activates the TTS process, leading to the translocation of ExoS and other TTS-effectors into the eukaryotic host cell (*2*).

ExoS includes an ADP-ribosyltransferase activity, which catalyzes the transfer of an ADP-ribose moiety from NAD to specific arginine residues of target proteins (*3*, *4*). In vitro studies have identified multiple substrates for ExoS ADPRT activity, including the cytoskeletal protein vimentin, soybean trypsin inhibitor, IgG_3, apolipoprotein A1, and the low molecular G- (LMWG-) proteins, Ras, RalA, Rab3, 4, 5, 7, 8, and 11, Rap1A and 2, Rac1, Cdc42, and RhoA, B, and D (*4*−*9*). The intracellular ADPRT substrate specificity of TTS-ExoS has been found to differ from that observed in vitro. Currently known cellular substrates of bacterially translocated ExoS ADPRT activity include the LMWG-proteins, H-Ras, N-Ras, and K-Ras, RalA, Rab5, 7, 8, and 11, Rac1, Cdc42, and the ERM family proteins, ezrin, radixin, and moesin (*8*−*12*). Notably, Rab4 and RhoA, B, and D, which are substrates of ExoS ADPRT activity in vitro, are not substrates of TTS-ExoS ADPRT activity. ExoS ADPRT-substrate specificity has also been found to vary in a cell line-dependent manner. For example, Rab proteins, Rac1 and Cdc42 are ADP-ribosylated by ExoS in human epithelial, endothelial, and fibroblastic cell lines but are not ADP-ribosylated in rodent cell lines or macrophages of either rodent or human origin (*13*, *14*). Together, the data support that the host cell directs the intracellular targeting of ExoS ADPRT activity after its TTS-mediated translocation.

Functional studies found that treatment of mammalian cells with ExoS-producing *Pa* strains results in inhibition of DNA synthesis, alterations in cytoskeletal structure, and over time a reduction in cell adherence and viability (*15*, *16*). Proteins within the Ras superfamily are involved in extracellular to intracellular signaling processes that can regulate cellular proliferation, differentiation, morphology, adherence, and apoptosis, providing an explanation for the diverse effects of ExoS on cell function. ExoS has also been found to exert different effects on LMWG-protein function, depending on

* Corresponding author. Mailing address: Department of Microbiology, Immunology and Cell Biology, Health Sciences North, P.O. Box 9177, West Virginia University, Morgantown, WV 26506. Phone: (304) 293-5843. Fax: (304) 293−7823. E-mail: jolson@hsc.wvu.edu.

[‡] Department of Pathology and Laboratory Medicine, Medical University of South Carolina.

[§] Departments of Cell and Molecular Pharmacology and Experimental Therapeutics, Medical University of South Carolina.

[||] Coastal Carolina University.

[⊥] College of Charleston.

[#] West Virginia University.

10.1021/bi0513554 CCC: $33.50
Published on Web 03/21/2006

the site (or sites) of ADP-ribosylation. The ADP-ribosylation of Ras by ExoS at Arg41 interferes with Ras GDP to GTP exchange, affecting Ras signaling processes (*10*, *17*, *18*). ExoS ADP-ribosylates RalA at three sites, with Arg52 being the preferred site, and interferes with RalA activation (*11*, *14*). In contrast to Ras and RalA, ExoS ADP-ribosylation of Rac1 leads to Rac1 activation, which reflects the preferred targeting of ExoS to Arg66 and Arg68 within the GAP region of Rac1 (*19*). Another recently identified family of cellular targets of TTS-ExoS ADPRT activity is the ERM proteins that influence cytoskeletal dynamics (*12*).

In vitro and cell culture studies support that ExoS ADPRT activity can target other eukaryotic cell proteins in addition to LMWG- and ERM proteins. Studies described in this paper used the bacterial−mammalian cell culture infection model (*15*), in conjunction with two-dimensional electrophoretic (2DE) analysis, to identify novel cellular substrates of TTS-ExoS ADPRT activity. In these analyses, a group of 17 kDa proteins was detected by 2DE in extracts of cells cocultured with ExoS producing *Pa*, but not in extracts from cells exposed to non-ExoS producing *Pa*. Analysis of the 17 kDa proteins by matrix-assisted laser desorption/ionization time-of-flight mass spectrometry (MALDI-TOF MS) and Western blotting identified the proteins as isoforms of cyclophilin A. CpA is a ubiquitous, predominantly cytosolic protein thought to be involved in protein folding, molecular chaperone functions, and signal transduction. The ADP-ribosylation of CpA by TTS-ExoS identifies CpA as another cellular target of ExoS ADPRT activity that works in concert to cause the cytopathic phenotype of ExoS in mammalian host cells.

MATERIALS AND METHODS

Materials. Difco reagents were used for bacterial culture (BD Biosciences, Franklin Lakes, NJ), and reagents for mammalian cell culture were obtained from Gibco-BRL (Gaithersburg, MD). All other chemicals and reagents were from Sigma-Aldrich (St. Louis, MO), except where indicated.

Bacterial Strains. P. aeruginosa strain 388 (*3*) and the isogenic ExoS mutant strain 388Δ*exoS* (*20*) were provided by Dara Frank (Medical College of Wisconsin, Milwaukee, WI). Bacteria were grown as described previously (*15*) at 37 °C in chelated tryptic soy broth dialysate medium, supplemented with 1% glycerol, 0.1 M monosodium glutamate, and 10 mM nitrilotriacetic acid. Prior to bacterial−eukaryotic cell coculture, late-log phase cultures of *Pa* strains were diluted to 10^7 or 10^8 cfu/mL in eukaryotic cell line-specific culture medium, supplemented with 0.6% bovine serum albumin (BSA).

Eukaryotic Cell Culture and Treatments. HT-29 colon (American Type Culture Collection, Manassas, VA, ATCC HTB-38) and T24 bladder (ATCC HTB-4) adenocarcinoma cells were cultured in McCoy's medium containing 10% fetal bovine serum, 100 units/mL penicillin, 100 μg/mL streptomycin (McCoy's-FBS) at 37 °C in 5% CO_2-95% air. For bacterial−eukaryotic cell coculture studies, eukaryotic cells were grown to approximately 80% confluency and then exposed to *Pa* strains at a MOI of 50 to 100 for 2, 4, or 6 h, as indicated. Other cell lines examined in these studies for comparison include CFT1 cells (*21*) (provided by Gerald Pier, Brigham & Women's Hospital, Harvard Medical School) and LNCaP cells (ATCC CRL-1740), which were cultured as previously described (*22*) or as specified by ATCC.

Identification of Cellular Targets of ExoS ADPRT Activity. Protein substrates of TTS-ExoS ADPRT activity were detected based on the transfer of radiolabeled ADP-ribose from intracellular NAD pools, radiolabeled using [2-^{3}H]-adenosine (21 Ci/mmol, GE Healthcare (formerly Amersham Biosciences), Piscataway, NJ). For these studies, HT-29 cells were seeded at 6×10^5 cells/mL in 6-well plates, cultured in McCoy's-FBS for 24 h, and serum starved in McCoy's 0.4% BSA for 8 h. Monolayers were then treated with 5 μg/mL actinomycin D for 30 min to inhibit RNA synthesis, washed, and incubated with 50 μCi/mL of [^{3}H]adenosine for 18 h. Monolayers were again washed and then cocultured with strains 388 or 388Δ*exoS* or no bacteria for 3 h. Cells were lysed in Laemmli sample buffer (*23*), and when indicated, further treated with 2 mg/mL RNase for 1 h at 37 °C. Samples were resolved by SDS−PAGE, fixed, treated with Amplify (GE Healthcare), dried, and analyzed by autoradiography.

Two-Dimensional Electrophoresis. 2DE analysis was performed according to previously described procedures (*24*, *25*). Following bacterial−eukaryotic coculture, cells were lysed and solubilized in 2DE lysis buffer [8 M urea, 2% Triton X-100, 0.3% dithiothreitol (DTT), and 0.5% Pharmalytes (Pfizer-Pharmacia, NY)]. Proteins were separated based on p*I* using immobilized pH gradient (IPG) isoelectric focusing (IEF) gel strips (Pfizer-Pharmacia or laboratory prepared) by focusing for 3 h at 300 V, followed by 21 h at 3500 V. The focused strips were equilibrated for 15 min in SDS equilibration buffer (50 mM Tris-HCl, pH 6.8, 6 M urea, 30% glycerol, 2% SDS) containing 20 mg/mL DTT, followed by 15 min with SDS equilibration buffer containing 25 mg/mL iodoacetamide. Proteins in the IPG strips were separated by size on 14−20% polyacrylamide gradient gels (*23*). Gels were silver stained (*26*), or proteins were transferred, using the method of Towbin et al. (*27*), to polyvinylidene fluoride (PVDF) membranes (Millipore, Bedford, MA), and immunoblotted for CpA using rabbit anti-cyclophilin A antibody (Upstate Biotechnology, Lake Placid, NY) and HRP-conjugated goat anti-rabbit IgG (Transduction Laboratories, San Diego, CA). Proteins were visualized by enhanced chemiluminescence (ECL) (GE Healthcare).

MALDI-TOF Mass Spectrometry. 2DE gels were stained using 0.1% Coomassie R-250, 40% ethanol, 10% acetic acid for 10 min and destained in a solution of 5% methanol and 7% acetic acid for 1 h. The protein spots were excised and destained three times in siliconized microfuge tubes with 700 μL of 1:1 (v/v) 10 mM ammonium bicarbonate/methanol and by rotation for 30 min. For dehydration, 700 μL of 10 mM ammonium bicarbonate was added to each tube for 1 h, followed by a brief wash with 700 μL of 1:1 (v/v) 10 mM ammonium bicarbonate/acetonitrile, and the addition of 700 μL of acetonitrile. After 15 min, the acetonitrile was removed, and the gel spots were dried in a Speed Vac for 30 min. Proteins were digested by the addition of 10 μL of 50 ng/μL trypsin in 10 mM ammonium bicarbonate. After 10 min, 60 μL of 10 mM ammonium bicarbonate was added, and reactions were allowed to proceed at 37 °C for 18 h. The trypsin digest supernatant was removed, and gels were extracted with 50 μL of 50% acetonitrile:5% formic acid

and sonication for 20 min, followed by the addition of 50 μL of 95% acetonitrile:5% formic acid and sonication for 20 min. The combined extract was dried in a Speed Vac. Protein samples were reconstituted in 3 μL of 50% acetonitrile, 0.5% trifluoroacetic acid (TFA). A 1 μL volume was removed from each sample and mixed 1:3 with 50 mM α-cyano-4-hydroxycinnamic acid in 70% acetonitrile, 0.1% TFA. A 1 μL volume of this mixture was then spotted onto a MALDI plate and analyzed by MALDI-TOF MS using a Voyager-DE MALDI mass spectrometer (PerSeptive Biosystems, Foster City, CA).

In Vitro ADP-Ribosylation of CpA by ExoS. In vitro ADPRT reactions were performed using recombinant CpA (BIOMOL, Plymouth Meeting, PA) and purified His-tagged ExoS (*28*). The 100 μL reaction mixture contained 200 mM Tris acetate, pH 6.0, 10 mM NAD, 68 nM 14-3-3 (the ExoS cofactor (*29*)), 1 μM CpA, and 10 or 40 nM ExoS, as indicated, with no ExoS added to negative control reactions. Reactions were incubated for 2 h at room temperature. Depending upon the method of analysis, reactions were terminated either by the addition of 4X Laemmli sample buffer and heating for 3 min at 95 °C (for SDS−PAGE analysis) or by the addition of 2DE lysis buffer (for 2DE analysis), or alternatively, samples were analyzed in a CpA *cis-trans*-isomerase assay or in a CpA co-immunoprecipitation (Co-IP) assay (as described below). In SDS−PAGE analyses, 20 μL of sample was resolved on 12% or 14% polyacrylamide gels, and proteins were visualized by Coomassie or silver staining. In 2DE analyses, the sample volume was increased to 180 μL with 2DE lysis buffer, and samples were loaded onto IPG strips and resolved by 2DE, as described above.

To monitor the incorporation of ADP-ribose into CpA, 2 μCi of nicotinamide adenine [adenylate-^{32}P] dinucleotide (^{32}P-NAD) (200 Ci/mmol, GE Healthcare) was added to 15 μL reaction mixtures containing 200 mM Tris acetate, 100 μM NAD, 10 nM ExoS, 150 ng of His-CpA or His-CpA mutant (see below), and 250 nM 14-3-3. The reaction was terminated with 4x Laemmli sample buffer and heating for 3 min at 95 °C, resolved by SDS−PAGE, and analyzed by autoradiography. The auto-ADP-ribosylation of ExoS served as a positive control in each reaction (*30*).

CpA Mutagenesis. The cDNA for CpA, including 5′ *Nde*I and 3′ *Bam*HI restriction enzyme sites, was generated by PCR using the I.M.A.G.E. Consortium Clone ID 4281376 (ATCC 6265707) as template and the forward primer, 5′-GGGAATTCCATATGGTCAACCCCACCG-3′, and reverse primer, 5′-GCAGCCGGATCCTTATTCGAGTTGTCCACAGTC-3′ (restriction sites are underlined). The PCR reaction conditions included denaturation for 2 min at 94 °C, followed by 35 cycles at 94 °C for 30 s, 62 °C for 30 s, 72 °C for 90 s, and a final extension at 72 °C for 10 min. The PCR product was digested with *Nde*I and *Bam*HI (New England Biolabs, Beverly, MA) and ligated into pET15b (Novagen, Madison, WI). The pET15b vector introduces an N-terminal 6xHis-tag, which was added to facilitate protein purification.

A PCR-based site-directed mutagenesis method (Strategene, La Jolla, CA) was used to generate arginine to lysine mutations in the *CpA* gene at residues encoding R55, R69, and R148. Oligonucleotides used for the mutagenesis were R55K, forward 5′-GTTCCTGCTTTCACAAAATTATTCCcGGGTTTATGTGTCAG-3′; R69K, forward 5′-GGGTGGTGACTTCACAAAACATAATGGCACTGGTG-3′; R148K, forward 5′-CATGGAGCGCTTTGGATCCAaGAATGGCAAGACCAG-3′; and their respective reverse complement primers. The PCR reaction conditions included denaturation for 5 min at 94 °C, followed by 18 cycles of 94 °C for 30 s, 60 °C for 30 s, 72 °C for 12 min, and a final extension at 72 °C for 60 min. The PCR reaction product was digested with 20 units of *Dpn*I (New England Biolabs), ethanol precipitated and electroporated into *Escherichia coli*, DH5α. Resultant colonies were screened by restriction enzyme analysis for introduction of the mutation, and CpA mutations were confirmed by DNA sequence analysis.

Expression of CpA Mutants. pET15b, encoding wild type (WT) His-CpA and His-CpA mutants, was isolated and electroporated into *E. coli* strain BL21(DE3) (Novagen) for protein production. Bacterial cultures were induced for protein expression with 1 mM IPTG, and bacteria were lysed either by passage through a French pressure cell (Thermo IEC, Needham Heights, MA) or chemically using Bacterial Protein Extraction Reagent (B-PER, Pierce Biotechnology, Rockford, IL). Following lysis, samples were centrifuged at 17000*g* at 4 °C. Subcellular analyses found that His-CpA resided and was the predominant protein within the cellular pellet. To isolate His-CpA and His-CpA mutants, the pellet was redissolved in 8 M urea, and residual precipitate was removed by centrifugation. CpA was subsequently found to be purified to near homogeneity by passage of the protein/urea mixture through a PD-10 column (GE Healthcare), equilibrated with PBS. This form of His-CpA, without further purification, was used in most analyses.

CpA Peptidyl-Prolyl Cis-trans-isomerase Enzymatic Assay. Recombinant His-CpA and ADP-ribosylated His-CpA peptidyl-prolyl *cis-trans*-isomerase activity was assessed spectrophotometrically using a chymotrypsin cleavable synthetic chromophore, *N*-succinyl-AAPF-*p*-nitroanilide. *N*-succinyl-AAPF-*p*-nitroanilide was prepared as a 2.5−10 mM stock solution in trifluoroethanol (TFE) with 470 mM LiCl. Enzymatic reactions were performed in a 1 mL reaction volume containing 33 mM HEPES, pH 7.8, 100 mM NaCl, 150 μg/mL chymotrypsin, and 12 nM of CpA, obtained from ADPRT reactions incubated with or without ExoS. The reaction mixture was chilled to 10 °C in a cuvette, and 250 μM of peptide was added and mixed quickly. Absorbance readings at 430 nm were collected every second for 5 min and analyzed using a Beckman DU 640 spectrophotometer (Fullerton, CA), equipped with an Auto 6 water cooled sampler accessory and a Brinkman water recirculation unit (Westbury, NY). All reactions were performed in duplicate, and the percentage of peptide in the cis conformation was determined prior to each experimental procedure using 75 μM peptide and 50 nM CpA. Enzymatic reactions containing 530 nM cyclosporin A (CsA) were included in analyses as a positive inhibition control.

CpA-calcineurin (CN) Co-immunoprecipitation Assay. To determine if ADP-ribosylation of CpA interfered with the ability of CpA or the CpA/CsA complex to bind to protein phosphatase PP2B (calcineurin), a co-immunoprecipitation (pull-down) reaction was performed using sepharose-GSH/GST-CpA coupled beads (GST-CpA) or ADP-ribosylated GSH/GST-CpA beads (GST-CpA-ADPRT). GST-CpA was generated by PCR as described in the CpA Mutagenesis

section using I.M.A.G.E. Consortium Clone ID 4281376 as template and the forward primer 5′-CGCGGATCCGTCAACCCCACCGTGTTC-3′ and reverse primer 5′-CCGAATTCTTATTCGAGTTGTCCACAGTC-3′ (restriction sites are underlined). The PCR product was digested with *Bam*HI and *Eco*RI (New England Biolabs) and ligated into pGEX-4T-1 (GE Healthcare). The pGEX-4T-1 vector introduces an N-terminal glutathione S-transferase (GST) sequence, which was added to facilitate protein pull-downs. GST-CpA beads were ADP-ribosylated in vitro as described above, using 200 nM ExoS and 100 ng/μL GST-CpA beads in a 350 μL reaction volume.

For the pull-down reactions, T24 cells were treated with or without 40 μM CsA, just prior to the addition of 10^7 cfu/mL strain 388 or 388Δ*exoS*, and cultured for 4 h. Bacteria were removed, and cells were lysed on ice for 20 min in Co-IP lysis buffer [30 mM HEPES, pH 7.5, 1% Triton X-100, 10 mM NaCl, 10% glycerol, 1 mM EGTA, 25 mM NaF, 1 mM Na_3VO_4, 10 mM β-glycerophospate, 1:1000 protease inhibitor cocktail (Sigma P8340)]. Lysates were cleared by centrifugation at 16000*g*, and the supernatant was incubated with 5 μg of GST-CpA or GST-CpA-ADPRT beads for 1 h at 4 °C. Beads were washed three times in lysis buffer, resuspended in Laemmli sample buffer, heated for 3 min at 95 °C, resolved by SDS−PAGE, and immunblotted for CN using rabbit anti-PP2B (Santa Cruz Biotechnology, Santa Cruz, CA), followed by HRP-conjugated anti-rabbit IgG (Sigma) and visualized by ECL.

RESULTS

Identification Cellular Targets of TTS-ExoS ADPRT Activity. The identification of cellular targets of TTS-ExoS ADPRT activity is technically difficult due to the lack of a direct means of detecting ADP-ribosylated proteins in intact cells. NAD, which is the source of ADP-ribose in the ADPRT reaction, is not membrane permeable. This precludes the use of radiolabeled NAD to identify ADP-ribosylated cellular substrates of TTS-ExoS ADPRT activity. Also, unlike phosphorylated proteins, no antibodies are commercially available to detect ADP-ribosylated proteins.

The approach we chose to identify cellular proteins ADP-ribosylated by ExoS was to radiolabel intracellular NAD pools using ^{3}[H]adenosine, then detect proteins labeled with ADP-ribose after coculture with *Pa* expressing ExoS. Since ^{3}[H]adenosine can be incorporated into multiple compounds within the cell, such as AMP, ADP, or ATP, as well as NAD, considerable background reactivity was associated with these analyses. Experimental variations introduced to help reduce this background included (i) serum starving cells, (ii) treatment with actinomycin D, prior to incorporation of ^{3}[H]-adenosine to inhibit RNA transcription, and (iii) treatment with RNase to further decrease RNA radiolabeling. These treatments led to the detection of at least 13 distinct bands in extracts of cells exposed to *Pa* strain 388, as compared to cells exposed to strain 388Δ*exoS* (Figure 1). ExoS substrates that have been identified are labeled. The focus of these studies was the 17 kDa radiolabeled protein.

Identification of 17 kDa ExoS ADP-Ribosylated Protein. A proteomic approach was used to identify the 17 kDa cellular target of ExoS ADPRT activity. We have previously shown that ADP-ribosylation of proteins causes a net acidic

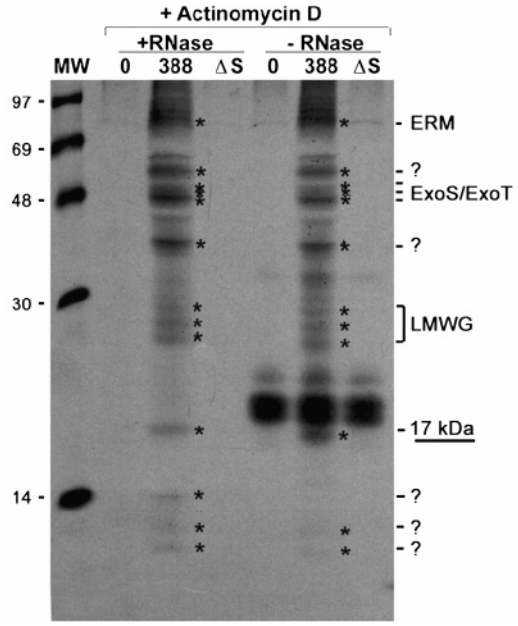

FIGURE 1: Analysis TTS-ExoS ADPRT cellular substrates. Serum starved HT-29 cells were treated for 30 min with 5 μg/mL actinomycin D, radiolabeled for 18 h with [^{3}H]adenosine, and cocultured for 3 h with ExoS producing strain 388 or strain 388Δ*exoS* (ΔS) or with no bacteria (0). Cells were lysed and when indicated treated for 1 h with 2 mg/mL RNase. ADPRT substrate modification was determined by autoradiography. Asterisks mark bands unique to TTS-ExoS treated cells.

shift in the p*I* of target proteins that is observable on 2DE gels (*8*, *10*). Consistent with ^{3}[H]adenosine radiolabeling studies in Figure 1, a series of four 17 kDa proteins were apparent in the p*I* range of 6.2−7.2 in 2DE analyses of lysates from HT-29 cells exposed to *Pa* strain 388, but not in lysates from cells exposed to strain 388Δ*exoS* (Figure 2A). Time-course analysis revealed that the appearance of the 17 kDa proteins required a 4 to 6 h coculture period, which is consistent with the time required for TTS-ExoS to ADP-ribosylate cellular substrates (Figure 2B). A similar alteration in 17 kDa protein mobility was observed in lysates of CFT1, LNCaP, and T24 cells in response to strain 388, indicating that this effect was not unique to the HT-29 cell line (data not shown).

To identify the 17 kDa proteins modified by ExoS, lysates from ADP-ribosylated cells were separated on 2DE gels, and three of the four protein spots (referred to as isoforms I−IV based on increasing p*I* in Figure 2A) were excised and digested in-gel with trypsin. The masses of the extracted peptides were determined by MALDI-TOF mass spectrometry, and a database search, using the MultiIdent (http://us.expasy.org/tools/multiident) search engine, revealed that cyclophilin A (CpA) closely matched 4 of the peptide masses in all three isoforms (739, 1381, 1834, and 1948) (Table 1A). To confirm whether the 17 kDa proteins were CpA, Western blots of 2DE gels were performed using CpA specific antiserum (Figure 3). In these analyses, broad, pH range 4−10, IPG IEF strips were used to allow the potential detection of parental (non-ADP-ribosylated) CpA. Four CpA spots, corresponding to apparent masses of 17 kDa and p*I*'s from 6.5 to 6.8, were observed in lysates of cells treated with strain 388, confirming that the four 17 kDa proteins were isoforms of CpA. Two additional isoforms of CpA, with a p*I* of 7.5 and 8.0, were also detected in lysates of

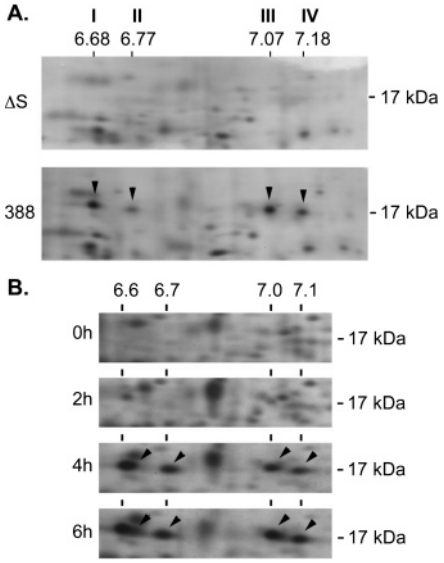

FIGURE 2: Alteration of 17 kDa proteins following exposure to ExoS-producing bacteria. (A) Detection of four 17 kDa proteins. Subconfluent HT-29 cells were cocultured with 10^8 cfu/mL strain 388 or 388Δ*exoS* (ΔS) for 4 h. Cells were lysed in 2DE lysis buffer and separated by p*I* using pH 6.2−7.2 IPG IEF strips, followed by SDS−PAGE on 14−20% polyacrylmide gradient gels. (B) Time-course analysis of appearance of 17 kDa proteins. HT-29 cells were exposed to strain 388 for 0, 2, 4, and 6 h. Lysates were prepared and resolved by 2DE as described in (A). Silver stained 2DE gels are shown. Black arrowheads indicate novel 17 kDa proteins. Apparent p*I* of isoforms I−IV and molecular mass are indicated.

cells treated with strain 388 or 388Δ*exoS*. The p*I* and mass of these latter two isoforms is consistent with their being parental, non-ADP-ribosylated CpA.

In Vitro ADP-Ribosylation of Recombinant CpA by ExoS. It was noticed in the above studies that the two parental CpA isoforms did not disappear with the appearance of modified isoforms (Figure 3). It therefore remained possible that the novel isoforms of CpA were induced by TTS-ExoS, but were not direct substrates of ExoS. To confirm that CpA was a substrate of ExoS ADPRT activity, in vitro ADPRT reactions were performed using recombinant human CpA and purified His-ExoS. As shown in Figure 4, recombinant, unmodified CpA presents as p*I* 7.8 and a more basic isoform on 2DE gels. Upon treatment with ExoS, the unmodified forms disappeared, and two new acidic isoforms, which have electrophoretic mobilities and p*I* equivalent to ADP-ribosylated isoforms I and III, appeared. This provides evidence that the appearance of two of the four CpA isoforms in *Pa* 388 coculture experiments (Figure 2) relates to the ADP-ribosylation of CpA by ExoS. The other CpA isoforms are suspected to represent posttranslational modifications of CpA, such as N-terminal acetylation, as discussed below.

Analysis of the Site of ADP-Ribosylation on CpA by ExoS. CpA isoforms I and II had identical trypsin digest peptide mass profiles, while the trypsin digests of isoform III yielded peptides that were shared by isoforms I and II, but also included peptides unique to isoform III (data not shown). This suggested that peptide differences might be due to posttranslational modification(s). In support of this possibility, tryptic peptide 1989 did not match predicted masses for CpA peptides, but the 1989 mass would be consistent with an acetylated N-terminus (1948 + 41) (Table 1A). Notably, subtraction for an ADP-ribose moiety (mass 541) did not allow matches of the unidentified peptides with CpA, precluding the direct identification of the site of ExoS ADP-ribosylation in CpA. ExoS ADP-ribosylates arginine residues on target proteins (*4*). Since the ADP-ribosylation of arginine residues is likely to prevent tryptic cleavage at these sites, we explored which arginine residues might be sites of ExoS ADP-ribosylation by comparing CpA peptides generated following digestion with chymotrypsin and trypsin (Table 1B). In these comparisons, peptides corresponding to those containing Arg19, Arg37, and Arg144 were found in both digests, ruling out these residues as sites of ADP-ribosylation. By deduction, this left Arg55, Arg69, and Arg148 as candidate sites for ExoS ADP-ribosylation.

Mutational Analysis of Sites of CpA ADP-Ribosylation by ExoS. To further investigate the ADP-ribosylation of CpA at sites Arg55, Arg69, or Arg148, His-tagged CpA and His-CpA R55K, R69K, and R148K mutants were constructed and tested for ADP-ribosylation by ExoS in vitro. Previous studies found LMWG-proteins to exhibit characteristic shifts in mobility by SDS−PAGE analyses in association with ADP-ribosylation by ExoS in vitro or within the cell (*8*). A shift in mobility of His-CpA was also detected by SDS−PAGE following ADP-ribosylation by ExoS in vitro (Figure 5A). Comparisons of the in vitro ADP-ribosylation of His-CpA by ExoS with that of the His-CpA mutants found the R148K mutant to exhibit a shift in mobility similar to that of WT CpA. This compared with a less efficient shift in mobility of the R55K and R69K His-CpA mutants, consistent with these mutations affecting the efficiency of ExoS ADP-ribosylation. Similar results were obtained using ^{32}P-NAD to examine the incorporation of radiolabeled ADP-ribose over time in in vitro ExoS ADPRT reactions. As shown in Figure 5B, efficient ADP-ribosylation of His-CpA and the His-CpA R148K mutant was detected after a 10 min reaction. However, ^{32}P-ADP-ribose incorporation was markedly reduced in His-CpA R55K and R69K mutants. The increase in auto-ADP-ribosylation of ExoS with time served as an internal control for each set of reactions. The results support that Arg55 and Arg69 in CpA function as sites of ExoS ADP-ribosylation.

Effects of ExoS ADP-Ribosylation on CpA Function. CpA is included among a large family of proteins, collectively referred to as immunophilins, which have peptidyl-prolyl *cis-trans*-isomerase (PPIase) activity and function as receptors for immunosuppressive drugs, such as cyclosporin A. While immunophilins have been identified in all organisms examined, including bacteria, fungi, animals, and plants, the physiological function of immunophilins is poorly understood. The lack of an understanding of the cellular function of CpA precludes directly assessing the cellular consequences of ExoS ADP-ribosylation of CpA. Alternatively, two approaches were used as a means of indirectly assessing the potential of ExoS ADP-ribosylation of CpA to alter cell function.

First, we examined the effect of ExoS ADP-ribosylation on CpA PPIase activity in an in vitro PPIase spectrophotometric assay. This assay was developed using a chymotrypsin-cleavable chromogenic peptide to follow the PPIase activity of CpA and ADP-ribosylated CpA. CsA, which binds to and inhibits CpA PPIase activity, was included as a positive inhibition control. ADP-ribosylation of CpA was found to reduce the amount of peptide conversion by 19%

Table 1: MALDI-TOF Mass Spectrometry Analysis of the 17 KDa Protein Peptide Fragments[a]

A. Trypsin Digest Masses (Average MH$^+$)

Observed	Theoretical	Difference	Residues	Sequence
739.56	737.79	1.77	31-36	TAENFR
1279.41	1279.47	-0.06	133-143	EGMNIVEAMER
1311.83	1311.47	0.36	133-143*	EGM*NIVEAM*ER
1381.68	1380.63	1.05	19-30	VSFELFADKVPK
1559.35	1558.81	0.54	55-68*	IIPGFM*CQGGDFTR
1834.16	1833.05	1.11	76-90	SIYGEKFEDENFILK
1948.03	1946.19	1.84	37-54	ALSTGEKGFGYKGSC*FHR
1948.95	1947.20	1.75	1-18	VNPTVFFDIAVDGEPLGR
1989.97	1989.23	0.73	1-18**	Ac-VNPTVFFDIAVDGEPLGR
2753.24	2752.09	1.15	91-117*	HTGPGILSM*ANAGPNTNGSQFFICTAI

B. Chymotrypsin Digest Masses (Average MH$^+$)

Observed	Theoretical	Difference	Residues	Sequence
1287.42	1286.43	0.99	36-47	RALSTGEKGFGY
1611.14	1609.82	1.32	22-35	ELFADKVPKTAENF
1624.09	1622.82	1.27	7-21	FDIAVDGEPLGRVSF
1872.70	1871.18	1.52	129-144*	GKVKEGM*NIVEAM*ERF
2594.57	2594.06	0.51	113-135*	ICTAKTEWLDGKHVVFGKVKEGM*

C. Sequence Coverage+

VNPTVFFDIA VDGEPLGRVS FELFADKVPK TAENFRALST GEKGFGYKGS CFHR**IIPGFM**
CQGGDFTRHN GTGGK**SIYGE KFEDENFILK HTGPGILSMA NAGPNTNGSQ FFICTAK**TEW
LDGKHVVFGK VK**EGMNIVEA MER**FGSRNGK TSKKITIADC GQLE

[a] *Oxidized methionine. **Acetylated N-terminus. +Bolded residues indicate sequences corresponding to peptides from trypsin digests, and underlined residues correspond to peptides from chymotrypsin digests. Arginine residues are shaded.

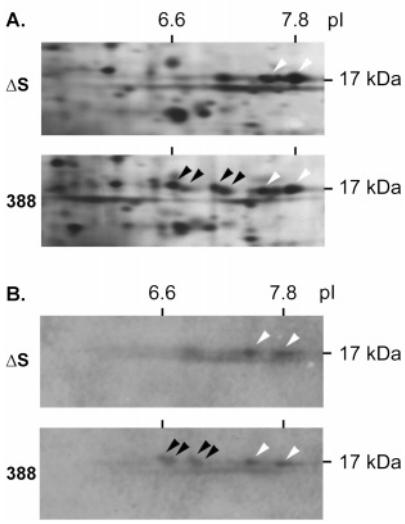

FIGURE 3: 2DE-Western blot identification of the 17 kDa proteins. HT-29 cells were cocultured with strain 388 or 388ΔS (ΔS) and analyzed by 2DE as described in Figure 2, except pH 4−10 IPG IEF strips were used. Two 2DE gels were performed in parallel and analyzed by (A) silver staining or (B) Western blotting, by transferring proteins to PVDF membranes and immunoblotting for cyclophilin A. White arrowheads indicate unmodified cellular CpA isoforms. Black arrowheads indicate novel CpA isoforms generated following exposure to ExoS producing bacteria. Apparent p*I* and molecular mass are indicated.

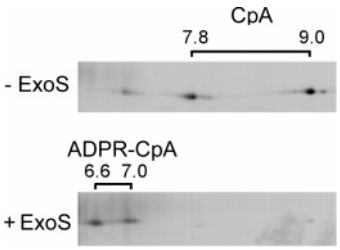

FIGURE 4: In vitro ADP-ribosylation of recombinant CpA using purified ExoS. Recombinant CpA (1 μM) was incubated with 40 nM ExoS (+ExoS) or without ExoS (−ExoS) for 2 h in an in vitro ADPRT reaction. The reaction was terminated by the addition of 2DE lysis buffer and was analyzed by 2DE as described in Figure 2, using pH 6−9 IPG IEF strips and 14% polyacrylamide gels.

after 60 s, which compared with a complete inhibition of CpA PPIase activity by CsA (Figure 6). ADP-ribosylated CpA used in these studies was evaluated by 2DE and found to be modified at both sites of ADP-ribosylation, indicating that the limited PPIase inhibition did not relate to inefficient CpA ADP-ribosylation. CsA binds to a region of CpA close to, but distinct from, its PPIase active site, which interferes with substrate binding and inhibits CpA PPIase activity. Since ADP-ribosylated CpA retained most of its PPIase activity, it is unlikely that ADP-ribosylation produces large structural changes in the catalytic region of the protein.

Second, we examined whether ExoS ADP-ribosylation disrupted CpA/CsA complex interaction with CN, a Ca^{2+}-calmodulin dependent protein phosphatase. The CpA/CsA complex is known to bind CN and inhibit its phosphatase activity in vitro and in vivo (*31*, *32*). CpA, alone, binds weakly to CN, but it is not yet clear whether this interaction is inhibitory or stimulatory (*33*). Mutating Arg69 in CpA to a neutral or acidic residue was found to cause a reduction (13-fold) in the effectiveness of CpA/CsA inhibition of CN (*34*). Since our studies support that Arg69 is a site of ADP ribosylation, we examined whether ADP-ribosylation of CpA might interfere with its interaction with CN using an in vitro pull-down reaction. In these studies, T24 cells were either treated with 40 μM CsA or treated with no drug, just prior to coculture with strain 388 or 388Δ*exoS*, and the binding of GST-CpA or GST-CpA-ADPRT to CN/PP2B was determined. As represented in the first panel in Figure 7, GST-CpA was able to pull-down PP2B in both strain 388 and 388Δ*exoS* treated cells, with this interaction being consistently more pronounced in 388 treated cells. One interpreta-

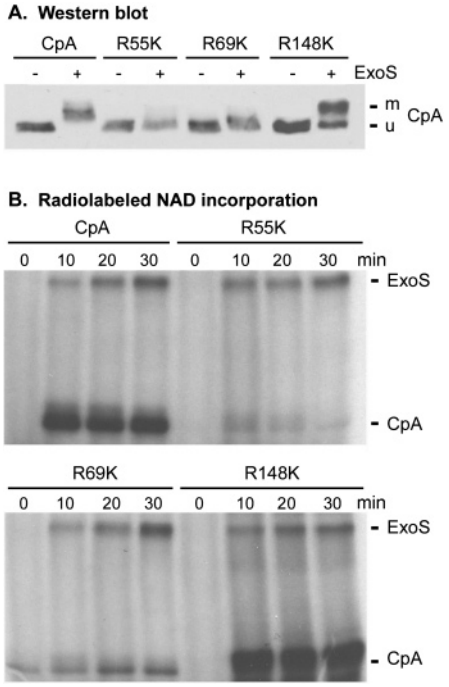

FIGURE 5: In vitro ADP-ribosylation of recombinant CpA mutants using purified ExoS. (A) Recombinant CpA, or CpA R55K, R69K, or R148K mutants (150 ng of each) were incubated without (−) or with 10 nM ExoS (+) in an in vitro ADPRT reaction. The reaction was terminated by the addition of 4X Laemmli sample buffer, and ADP-ribosylation was analyzed based on the shift in CpA mobility by SDS−PAGE and Western blot analysis. ADP-ribose modified (m) and unmodified (u) CpA are labeled. (B) Time course in vitro ExoS ADPRT reactions were performed as in (A), but including 2 μCi of ^{32}P NAD to assess the incorporation of radiolabed ADP-ribose into CpA. Reactions were performed in the absence of ExoS (0) or in the presence of ExoS for 10, 20, and 30 min. The reaction was terminated with 4X Laemmli sample buffer, resolved by SDS−PAGE, and visualized by autoradiography. Auto-ADP-ribosylated ExoS and CpA are labeled. Auto-ADP-ribosylated ExoS served as an internal control in these studies for monitoring the relative increase in incorporation of radiolabeled ADP-ribose with time.

tion of the latter finding is that ADP-ribosylation of CpA in 388 treated cells blocks endogenous CpA binding to PP2B, increasing the availability of PP2B to bind to the GST-CpA pull-down probe. In the second panel in Figure 7, treatment of cells with CsA was found to have minimal effect on GST-CpA binding to PP2B. In contrast, as shown in the third panel of Figure 7, ExoS ADP-ribosylation of GST-CpA probe, prior to its incubation with cell lysates, severely inhibited its ability to bind to cellular PP2B. The studies support that ExoS ADP-ribosylation can affect CpA function by interfering with its ability to interact with CN/PP2B phosphatase.

DISCUSSION

ExoS is among the virulence factors utilized by *Pa* to promote the infectious process. TTS-ExoS is able to exert diverse effects on eukaryotic cell function that alter cell growth, cytoskeletal structure, and adherence properties. The diverse cellular effects of ExoS relate to it having both GAP and ADPRT activities, and to the ability of these activities to target multiple eukaryotic cell proteins. ExoS GAP activity targets LMWG-proteins in the Rho family (*35*, *36*), and, while the substrate specificity of ExoS ADPRT activity has not been completely elucidated, it is currently known to target LMWG-proteins in the Ras and Rho families and ERM

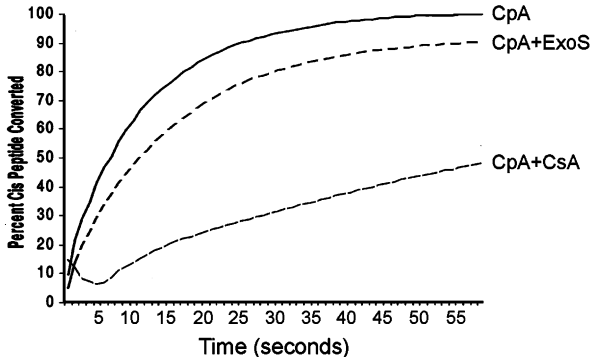

FIGURE 6: Effect of ExoS ADP-ribosylation of CpA on PPIase activity. CpA or ADP-ribosylated CpA was examined for peptidyl-propyl *cis-trans*-isomerase activity in a spectrophotometeric assay using a chymotrypsin cleavable synthetic peptide chromophore, *N*-succinyl-AAPF-*p*-nitroanilide. Enzymatic reactions contained 12 nM CpA, 40 nM ExoS or no ExoS, 250 μM peptide, and 150 μg/mL chymotrypsin. Absorbance readings were obtained every 5 s, and all reactions were performed in duplicate. Samples containing 530 nM cyclosporin (CsA) served as a positive control for CpA PPIase inhibition and produced readings equivalent to controls without CpA. A single assay representative of multiple assays is shown. (CpA Vo = 2.4 ± 0.4; CpA+ExoS Vo = 1.9 ± 0.6; CpA+CsA Vo = 0.4.)

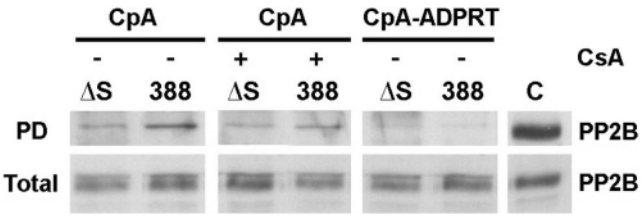

FIGURE 7: Effect of ExoS ADP-ribosylation of CpA on its interaction with CN/PP2B. T24 cells were treated with or without 40 μM of CsA (+ or −) just prior to a 4 h coculture period with strain 388 or 388Δ*exoS* (ΔS). Bacteria were removed, cells were lysed, and CpA was examined for its ability to interact with endogenous CN/PP2B in pull-down reactions using 5 μg of GST-CpA (CpA) or ADP-ribosylated GST-CpA (CpA-ADPRT) beads. Beads were washed, resuspended in Laemmli sample buffer, resolved by SDS−PAGE, and immunoblotted for CN using rabbit anti-PP2B, followed by HRP-conjugated anti-rabbit IgG. CN/PP2B associating with CpA or CpA-ADPRT beads (PD), relative to total PP2B, and a PP2B control (C) are shown.

family proteins (*8*, *9*, *11*, *12*, *28*). Studies comparing the coordinate function of the GAP and ADPRT activity of TTS-ExoS found the ADPRT activity to be responsible for the severe effects of ExoS on cell morphology, growth, and adherence (*19*, *37*). Alternatively, ExoS-GAP activity was linked to the anti-phagocytic function of ExoS in J774A.1 macrophages (*14*). Although ExoS GAP and ADPRT activities have been extensively studied, the precise mechanism by which ExoS causes its diverse effects on eukaryotic cell function remains unclear.

To further elucidate the cellular mechanism of ExoS, bacterial−eukaryotic cell coculture studies using cells with metabolically radiolabeled NAD were performed to assess the potential cellular substrate repertoire of TTS-ExoS ADPRT activity. In these analyses, a minimum of thirteen distinct ADP-ribose radiolabeled protein bands was detected, which included bands that correspond to ERM proteins (*12*), auto-ADP-ribosylated ExoS (*30*), multiple LMWG-proteins (*8*, *9*, *11*, *28*), and at least six other unidentified proteins. Our focus was the 17 kDa ExoS ADP-ribosylated substrate.

In initial studies using 2DE to monitor the ADP-ribosylation of the 17 kDa protein by *Pa*-TTS-ExoS, four protein spots were apparent in cell lysates in the p*I* range of 6.6 to 7.1. Kinetic analysis revealed that the 17 kDa spots required a minimum 4 h exposure to ExoS producing bacteria for detection, which is consistent with the 17 kDa protein being a later target of TTS-ExoS ADPRT activity during the *Pa* infectious process. It should also be noted though that at this time in our studies it was unclear whether the appearance of the 17 kDa spots was the result of TTS-ExoS ADP-ribosylation of constitutive proteins, or related to new protein synthesis or posttranslational modifications induced by ExoS.

To further clarify the origin of the 17 kDa spots, 3 of the 4 spots were excised, digested with trypsin, and analyzed by MALDI-TOF-MS. The peptide maps of spots I and II were identical, while spot III yielded both shared and unique peptide masses. Further characterization of all four spots through analyses of peptide digests supported that all 4 spots were the same protein, determined based on a protein database search to be cyclophilin A. The identity of the 4 spots as isoforms of CpA was confirmed by Western blot analyses. CpA has previously been characterized as several isoforms within the cell, with apparent p*I*'s ranging from 6.4 to 8.1 (SWISS-2DPAGE accession number P05092; http://au.expasy.org/ch2d). 2DE Western blot analysis using a broad p*I* (pH 4−10) range, revealed 7.5 and 8.0 isoforms of CpA in both strain 388-treated and control cell lysates. These results are consistent with the two predominate cellular isoforms of CpA, at p*I* 7.5 and 8.0, being ADP-ribosylated by ExoS at two sites, producing CpA isoforms I−IV. The continued presence of the 7.5 and 8.0 CpA isoforms in cells exposed to TTS-ExoS indicated that only a subset of CpA was being ADP-ribosylated by TTS-ExoS.

In further support of CpA functioning as a cellular target of ExoS, in vitro ExoS ADPRT reactions using purified CpA and ExoS found CpA to shift in p*I* in an identical manner as CpA isoforms I and III detected in bacterial coculture experiments. The detection of four ADP-ribosylated CpA isoforms in coculture experiments, as compared to two isoforms detected in vitro ADPRT reactions, can be explained by the previously reported posttranslational glycosylation and N-terminal acetylation of CpA (*38*−*40*). It was also of interest to examine why CpA ADP-ribosylation within the cell did not reach completion. To assess whether a cellular component might be preventing or inhibiting ExoS ADP-ribosylation of CpA, HT-29 lysates were ADP-ribosylated by recombinant ExoS in vitro and analyzed by 2DE. In these studies, the p*I* 7.5 and 8.0 isoforms of CpA were found to disappear in ExoS-treated lysates in association with the appearance of isoforms I−IV, indicating that no soluble cellular factor was interfering with the ADPRT reaction (data not shown). A limitation of this approach is that it does not rule out the possibility that cellular architecture or another cellular constraint might be preventing TTS-ExoS from interacting with subpopulations of CpA. In this regard, CpA has been found to be translocated into the nucleus when bound to zinc (*41*), which may make this subpopulation of CpA inaccessible to TTS-ExoS. Another factor that might influence the efficiency of CpA ADP-ribosylation by ExoS is that CpA is predominately a cytosolic protein (*42*, *43*), and ExoS has been found to localize and preferentially target membrane associated substrates (*44*). CpA has been documented to associate with cellular membranes in the renal cortex, and membrane disassociation occurs upon interaction with CsA or a substrate of CpA PPIase activity (*45*). Together these findings support the notion that the limited efficiency of CpA ADP-ribosylation by ExoS within the cell may reflect the accessibility of only a subpopulation of CpA, possibly membrane associated, to TTS-ExoS.

A comparison of peptide maps of CpA and ADP-ribosylated CpA did not reveal any peptide masses suggestive of ADP-ribosylation, precluding the direct identification of the site(s) on CpA ADP-ribosylated by TTS-ExoS. ExoS is known to ADP-ribosylate arginine residues within substrates (*4*) and comparisons of peptide masses from trypsin and chymotrypsin digests eliminated Arg19, Arg37, and Arg144 as sites of ADP-ribosylation. Using site-directed mutagenesis to examine whether the remaining arginine residues, Arg55, Arg69, and Arg148, were sites of ExoS ADP-ribosylation, in vitro ADPRT reactions found the R55K and R69K CpA mutants to be less efficiently ADP-ribosylated by ExoS than WT CpA or R148K CpA mutant.

Sites of ADP-ribosylation detected in vitro generally correspond to preferred sites of ADP-ribosylation within the cell (*11*, *46*). To further explore the possibility that Arg55 and Arg69 in CpA were sites of ExoS ADP-ribosylation, specific CpA functional assays were performed. Structural and functional studies support the role of Arg55 in the peptidyl-propyl *cis-trans*-isomerase reaction of CpA (*47*, *48*). Using an in vitro PPI isomerase reaction to examine whether Arg55 function is affected by ExoS ADP-ribosylation, a 19% reduction in CpA PPIase activity was detected following in vitro ExoS ADPRT reactions. This reduction was much less than that observed in CpA R55K mutational studies, where only 1% of CpA PPI activity was retained (*47*). The modest inhibition in PPIase activity would support that Arg55 is not the preferred site of ExoS ADP-ribosylation. The other site of ExoS ADP-ribosylation on CpA, Arg69, appears to function in interactions presenting CsA for CN phosphatase inhibition (*34*). When GST-CpA or ADP-ribosylated GST-CpA pull-down assays were performed to assess if ExoS ADP-ribosylation affected its ability to interact with CN/PP2B, both cellular and in vitro analyses supported that ExoS ADP-ribosylation interfered with CpA binding to CN/PP2B. The efficiency of this inhibition is consistent with Arg69 being a preferred target of ExoS ADP-ribosylation, and supports the potential of ExoS ADP-ribosylation to alter CpA function by interfering with CpA-cellular protein interactions.

As with other immunophilins, an understanding of the cellular function of CpA remains limited. CpA is generally viewed as a housekeeping protein involved in chaperone-like functions, and important for proper protein folding. Consistent with this role, CpA production has been shown to be upregulated in cells in response to heat stress, hypoxia, and exposure to heavy metals (*49*, *50*). CpA has also been shown to be an essential component of a heat-shock protein−immunophilin chaperone complex involved in the transport of newly synthesized cholesterol (*51*). One of the best characterized functions of CpA is its binding to the immunosuppressive drug, CsA, which in T-cells suppresses mitogen-activated proliferation through inhibition of CN/PP2B (*32*, *52*, *53*). Interestingly, while CpA/CsA complex inhibition of CN phosphatase activity in T-cells has been well studied, little is known about the involvement of CpA

in this pathway in the absence of CsA. Less well-characterized activities of CpA include a calcium dependent nuclease activity, that is associated with apoptosis in rat thymocytes (*54*), and a zinc dependent binding to DNA in macrophages, which has as yet unknown physiological consequences (*41*). Each of these proposed functions implicates the involvement of CpA−protein interactions in the cellular role of CpA. The evidence that ExoS ADP-ribosylation of CpA has a modest effect on its enzymatic activity, but efficiently inhibits CpA interaction with CN/PP2B, suggests that the more significant functional consequence of CpA ADP-ribosylation relates to its potential to interfere with CpA-protein interactions.

The identification of the predominantly cytosolic protein, CpA, as a cellular substrate of TTS-ExoS was an unexpected finding. All other identified cellular targets of ExoS ADPRT activity are proteins that mediate signal transduction, and their modification by ExoS has the potential to produce cellular changes that are beneficial to the *Pa* infectious process. Interestingly, of the identified cellular targets of TTS-ExoS ADPRT activity, only subtle effects on protein function occur in association with ExoS ADP-ribosylation, and no known target yet accounts for the observed effects of ExoS on cell function (*11*, *12*, *19*, *46*). The targeting by ExoS to a housekeeping protein, such as CpA, and the potential of ExoS ADP-ribosylation to interfere with CpA−protein interactions adds another level of complexity to the generalized cellular effects of ExoS. In this regard, as an understanding of the cellular targeting of ExoS ADPRT activity progresses, a picture unfolds of a versatile toxin that can facilitate *Pa* survival through the targeting and interruption of multiple host cell processes, and the importance of specific targets will vary depending on the eukaryotic cell environment.

ACKNOWLEDGMENT

We would like to thank Dara Frank for the bacterial strains used in these studies and Gerald Pier for the CFT1 cells and his assistance with the culturing of these cells. We would also like to acknowledge the contribution of Elizabeth Rucks, Deanne Vincent, and Kristy Johnson to this project. This work was supported by Public Health Services Grant NIH-NIAID 45569, by the Medical University of South Carolina Institutional Research Funds, and by the Mary C. Babb Cancer Center Foundation Fund 2V882 from West Virginia University.

REFERENCES

1. Bodey, G. P., Bolivar, R., Fainstein, V., and Jadeja, L. (1983) Infections caused by *Pseudomonas aeruginosa*, *Rev. Infect. Dis. 5*, 270−313.
2. Yahr, T. L., Goranson, J., and Frank, D. W. (1996) Exoenzyme S of *Pseudomonas aeruginosa* is secreted by a type III pathway, *Mol. Microbiol. 22*, 991−1003.
3. Iglewski, B. H., Sadoff, J., Bjorn, M. J., and Maxwell, E. S. (1978) *Pseudomonas aeruginosa* exoenzyme S: an adenosine diphosphate ribosyltransferase distinct from toxin A, *Proc. Natl. Acad. Sci. U.S.A. 75*, 3211−3215.
4. Coburn, J., Wyatt, R. T., Iglewski, B. H., and Gill, D. M. (1989) Several GTP-binding proteins, including $p21^{c-H-ras}$, are preferred substrates of *Pseudomonas aeruginosa* exoenzyme S, *J. Biol. Chem. 264*, 9004−9008.
5. Coburn, J., and Gill, D. M. (1991) ADP-ribosylation of $p21^{ras}$ and related proteins by *Pseudomonas aeruginosa* exoenzyme S, *Infect. Immun. 59*, 4259−4262.
6. Bette-Bobillo, P., Giro, P., Sainte-Marie, J., and Vidal, M. (1998) Exoenzyme S from *P. aeruginosa* ADP-ribosylates rab4 and inhibits transferrin recycling in SLO-permeabilized reticulocytes, *Biochem. Biophys. Res. Commun. 244*, 336−341.
7. Riese, M. J., Wittinghofer, A., and Barbieri, J. T. (2001) ADP-ribosylation of Arg41 of Rap by ExoS inhibits the ability of Rap to interact with its guanine nucleotide exchange factor, C3G, *Biochemistry 40*, 3289−3294.
8. Fraylick, J. E., Rucks, E. A., Greene, D. M., Vincent, T. S., and Olson, J. C. (2002) Eukaryotic cell determination of ExoS ADP-ribosyltransferase substrate specificity, *Biochem. Biophys. Res. Commun. 291*, 91−100.
9. Henriksson, M. L., Sundin, C., Jansson, A. L., Forsberg, A., Palmers, R. H., and Hallberg, B. (2002) Exoenzyme S shows selective ADP-ribosylation and GTP-ase activating protein (GAP) activities towards small GTPases in vivo, *Biochem. J. 367*, 617−628.
10. Vincent, T. S., Fraylick, J. E., McGuffie, E. M., and Olson, J. C. (1999) ADP-ribosylation of oncogenic Ras proteins by *Pseudomonas aeruginosa* exoenzyme S in vivo, *Mol. Microbiol. 32*, 1043−1053.
11. Fraylick, J. E., Riese, M. J., Vincent, T. S., Barbieri, J. T., and Olson, J. C. (2002) ADP-ribosylation and functional effects of *Pseudomonas* exoenzyme S on cellular RalA, *Biochemistry 41*, 9680−9687.
12. Maresso, A. W., Baldwin, M. R., and Barbieri, J. T. (2004) ERM proteins are high affinity targets for ADP-ribosylation by *P. aeruginosa* ExoS, *J. Biol. Chem. 279*, 38402−38408.
13. Rucks, E. A., Fraylick, J. E., Brandt, L. M., Vincent, T. S., and Olson., J. C. (2003) Cell line differences in bacterially translocated ExoS ADP-ribosyltransferase substrate specificity, *Microbiology 149*, 319−331.
14. Rocha, C. L., Coburn, J., Rucks, E. A., and Olson, J. C. (2003) Characterization of *Pseudomonas aeruginosa* exoenzyme S as a bifunctional enzyme in J774A.1 macrophages, *Infect. Immun. 71*, 5296−5305.
15. Olson, J. C., McGuffie, E. M., and Frank, D. W. (1997) Effects of differential expression of the 49-kilodalton exoenzyme S by *Pseudomonas aeruginosa* on cultured eukaryotic cells, *Infect. Immun. 65*, 248−256.
16. Olson, J. C., Fraylick, J. E., McGuffie, E. M., Dolan, K. M., Yahr, T. L., Frank, D. W., and Vincent, T. S. (1999) Interruption of multiple cellular processes in HT-29 epithelial cells by *Pseudomonas aeruginosa* exoenzyme S, *Infect. Immun. 67*, 2847−2854.
17. Ganesan, A. K., Vincent, T. S., Olson, J. C., and Barbieri, J. T. (1999) *Pseudomonas aeruginosa* exoenzyme S disrupts Ras-mediated signal transduction by inhibiting guanine nucleotide exchange factor catalyzed nucleotide exchange, *J. Biol. Chem. 274*, 21823-21829.
18. Henriksson, M. L., Rosqvist, R., Telepnev, M., Wolf-Watz, H., and Hallberg, B. (2000) Ras effector pathway activation by epidermal growth factor is inhibited in vivo by exoenzyme S ADP-ribosylation of Ras, *Biochem. J. 347*, 217−222.
19. Rocha, C. L., Rucks, E. A., Greene, D. M., and Olson, J. C. (2005) Examination of the coordinate effects of *Pseudomonas* ExoS on Rac1, *Infect. Immun. 73*, 5458−5467.
20. Kulich, S. M., Frank, D. W., and Barbieri, J. T. (1995) Expression of recombinant exoenzyme S of *Pseudomonas aeruginosa*, *Infect. Immun. 63*, 1−8.
21. Yankaskas, J. R., Haizlip, J. E., Conrad, M., Koval, D., Lazarowski, E., Paradiso, A. M., Rinehart, C. A. J., Sarkadi, B., Schlegel, R., and Boucher, R. (1993) Papilloma virus immortalized tracheal epithelial cells retain a well differentiated phenotype, *Am. J. Physiol. Cell Physiol. 264*, C1219−C1230.
22. McGuffie, E. M., Fraylick, J. E., Vincent, T. S., and Olson, J. C. (1999) Differential sensitivity of human epithelial cells to *Pseudomonas aeruginosa* exoenzyme S, *Infect. Immun. 67*, 3494−3503.
23. Laemmli, U. K. (1970) Cleavage of structural proteins during the assembly of the head of bacteriophage T4, *Nature 227*, 680−685.
24. Gorg, A., Postel, W., and Gunther, S. (1988) The current state of two-dimensional electrophoresis with immobilized pH gradients, *Electrophoresis 9*, 531−546.
25. Dunn, M. J., and Corbett, J. M. (1996) Two-dimensional polyacrylamide gel electrophoresis, *Methods Enzymol. 271*, 177−203.
26. Blum, H., Beier, H., and Gross, H. J. (1987) Improved silver staining of plant proteins, RNA, and DNA in polyacrylamide gels, *Electrophoresis 8*, 93−99.

27. Towbin, H., Staehelin, T., and Gordon, J. (1979) Electrophoretic transfer of proteins from polyacrylamide gels to nitrocellulose sheets: procedure and some applications, *Proc. Natl. Acad. Sci. U.S.A. 76*, 4350−4354.
28. McGuffie, E. M., Frank, D. W., Vincent, T. S., and Olson, J. C. (1998) Modification of Ras in eukaryotic cells by *Pseudomonas aeruginosa* exoenzyme S, *Infect. Immun. 66*, 2607−2613.
29. Fu, H., Coburn, J., and Collier, R. J. (1993) The eukaryotic host factor that activates exoenzyme S of *Pseudomonas aeruginosa* is a member of the 14-3-3 protein family, *Proc. Natl. Acad. Sci. U.S.A. 90*, 2320−2324.
30. Riese, M. J., Goehring, U.-M., Ehrmantraut, M. E., Moss, J., Barbieri, J. T., Aktories, K., and Schmidt, G. (2002) Auto-ADP-ribosylation of *Pseudomonas aeruginosa* ExoS, *J. Biol. Chem. 277*, 12082−12088.
31. Liu, J., Farmer, J. D. J., Lane, W. S., Friedman, J., Weissman, I., and Schreiber, S. L. (1991) Calcineurin is a common target of cyclophilin-cyclosporin A and FKBP-FK506 complexes, *Cell 66*, 807−815.
32. Schreiber, S. L., and Crabtree, G. R. (1992) The mechanism of action of cyclosporin A and FK506, *Immunol. Today 13*, 136−142.
33. Cardenas, M. E., Hemenway, C., Muir, R. S., Ye, R., Fiorentino, D., and Heitman, J. (1994) Immunophilins interact with calcineurin in the absence of exogenous immunosuppressive ligands, *EMBO J. 13*, 5944−5957.
34. Etzkorn, F. A., Change, Z. Y., Stolz, L. A., and Walsh, C. T. (1994) Cyclophilin residues that affect noncompetitive inhibition of the protein serine phosphatase activity of calcineurin by the cyclophilin-cyclosporin A complex, *Biochemistry 33*, 2380−2388.
35. Goehring, U.-M., Schmidt, G., Pederson, K. J., Aktories, K., and Barbieri, J. T. (1999) The N-terminal domain of *Pseudomonas aeruginosa* exoenzyme S is a GTPase activating protein for Rho-GTPases, *J. Biol. Chem. 274*, 36369−36372.
36. Pederson, K. J., Vallis, A. J., Aktories, K., Frank, D. W., and Barbieri, J. T. (1999) The amino-terminal domain of *Pseudomonas aeruginosa* ExoS disrupts actin filaments via small-molecular-weight GTP-binding proteins, *Mol. Microbiol. 32*, 393−401.
37. Fraylick, J. E., La Rocque, J. R., Vincent, T. S., and Olson, J. C. (2001) Independent and coordinate effects of ADP-ribosyltransferase and GTPase-activating activities of exoenzyme S on HT-29 epithelial cell function, *Infect. Immun. 69*, 5318−5328.
38. Hirtzlin, J., Farber, P. M., Franklin, R. M., and Bell, A. (1995) Molecular and biochemical characterization of a *Plasmodium falciparum* cyclophilin containing a cleavable signal sequence, *Eur. J. Biochem. 232*, 765−772.
39. Misumi, S., Fuchigami, T., Takamune, N., Takahashi, I., Takama, M., and Shoji, S. (2002) Three isoforms of cyclophilin A associated with human immunodeficiency virus type 1 were found by proteomics by using two-dimensional gel electrophoresis and matrix-assisted laser desorption ionization-time of flight mass spectrometry, *J. Virol. 76*, 10000−10008.
40. Rautajoki, K., Nyman, T. A., and Lahesmaa, R. (2004) Proteome characterization of human T helper 1 and 2 cells, *Proteomics 4*, 84−92.
41. Krummrei, U., Bang, R., Schmidtchen, R., Brune, K., and Bang, H. (1995) Cyclophilin A is a zinc-dependent DNA binding protein in macrophages, *FEBS Lett. 371*, 47−51.
42. Thalhammer, T., Kieffer, L. T., Jiang, T., and Handschumacher, R. E. (1992) Isolation and partial characterization of membrane-associated cyclophilin and a related 22-kDa glycoprotein, *Eur. J. Biochem. 206*, 31−37.
43. Gothel, S. F., and Marahiel, M. A. (1999) Peptidyl-prolyl cis-trans isomerases, a superfamily of ubiquitous folding catalysts, *Cell. Mol. Life Sci. 55*, 423−436.
44. Pederson, K. J., Pal, S., Vallis, A. J., Frank, D. W., and Barbieri, J. T. (2000) Intracellular localization and processing of *Pseudomonas aeruginosa* ExoS in eukaryotic cells, *Mol. Microbiol. 37*, 287−299.
45. Demeule, M., Laplante, A., Sepehr-Arae, A., Murphy, G. M., Wenger, R. M., and Beliveau, R. (2000) Association of cyclophilin A with renal brush border membranes: redistribution by cyclosporine A, *Kidney Int. 57*, 1590−1598.
46. Ganesan, A. K., Frank, D. W., Misra, R. P., Schmidt, G., and Barbieri, J. T. (1998) *Pseudomonas aeruginosa* exoenzyme S ADP-ribosylates Ras at multiple sites, *J. Biol. Chem. 273*, 7332−7337.
47. Zydowsky, L. D., Etzkorn, F. A., Chang, H. Y., Ferguson, S. B., Stolz, L. A., Ho, S. I., and Walsh, C. T. (1992) Active site mutants of human cyclophilin A separate peptidyl-prolyl isomerase activity from cyclosporin A binding and calcineurin inhibition, *Protein Sci. 1*, 1092−1099.
48. Zhao, Y., and Ke, H. (1996) Crystal structure implies that cyclophilin predominantly catalyzes the trans to cis isomerization, *Biochemistry 35*, 7356−7361.
49. Andreeva, L., Motterlini, R., and Green, C. J. (1997) Cyclophilins are induced by hypoxia and heat stress in myogenic cells, *Biochem. Biophys. Res. Commun. 237*, 6−9.
50. Sturzenbaum, S. R., Morgan, A. J., and Kille, P. (1999) Characterization and quantification of earthworm cyclophilins: identification of invariant and heavy metal responsive isoforms, *Biochim. Biophys. Acta 1489*, 467−473.
51. Uittenbogaard, A., Ying, Y., and Smart, E. J. (1998) Characterization of a cytosolic heat-shock protein-caveolin chaperone complex. Involvement in cholesterol trafficking, *J. Biol. Chem. 273*, 6525−6532.
52. Gordon, D., and Nouri, A. M. (1981) Comparison of the inhibition by glucocorticosteroids and cyclosporin A of mitogen-stimulated human lymphocyte proliferation, *Clin. Exp. Immunol. 44*, 287−294.
53. Kumagai, N., Benedict, S. H., Mills, G. B., and Gelfand, E. W. (1988) Cyclosporin A inhibits initiation but not progression of human T cell proliferation triggered by phorbol esters and calcium ionophores, *J. Immunol. 141*, 3747−3752.
54. Montague, J. W., Gaido, M. L., Frye, C., and Cidlowski, J. A. (1994) A calcium-dependent nuclease from apoptotic rat thymocytes is homologous with cyclophilin. Recombinant cyclophilins A, B, and C have nuclease activity, *J. Biol. Chem. 269*, 18877−18880.

BI0513554